Ambisonic Synthesis of Complex Sources

Dylan Menzies
Marwan Al-Akaidi
De Montfort University

December 27, 2006

Abstract

We show how exterior expansions of complex sound sources are flexible objects for producing Ambisonic soundfield encodings. The sources can be synthesized or recorded directly, rotated and positioned in space. Related techniques can also be used to efficiently add high quality reverberation depending on the orientation and location of the source and listener.

1 Introduction

Real soundfields are frequently the result of sound from numerous sound sources, each localized to a well defined region. Synthesizing these using speaker-based and binaural approaches is a natural goal. Good results have been achieved for distant sources, which reach the listener as plane waves. Distance perception can be simulated using distance filtering and reverberation balance. It is also possible in low-order Ambisonic systems,[1, 2], to approximately synthesize a diffuse source at varying distance, [3, 4], which can be useful in a creative setting. Soundfield synthesis of an object with non-uniform directivity has been considered in the farfield using spherical harmonic representation, [3, 4]. With the development of high-order acoustic field construction, the simulation of nearfield sources becomes feasible. This has been developed for a monopole source in the context of high-order Ambisonics by reconstructing a monopole field about the listener, [5]. Using

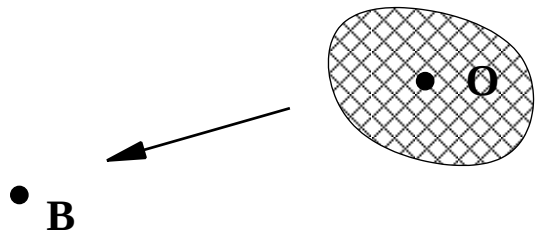

Figure 1: Overall scheme. O denotes the extended source object, and B the listener.

the wavefield approach,[6, 7], the directional properties of objects have been encoded with filters that feed the speaker array directly, [8, 9].

A localized source typically differs in two respects from simple monopole source. The sound radiates from a region of non-zero width, and the directivity of radiation is not uniform. Near to the object the soundfield will be reactive, like a monopole's, but possibly have a much more complex geometry. We should fully expect this added richness to be exploited by the auditory system for its information content, and so to have perceptual significance. Although this does not appear to have been studied in detail, informal listening provides strong evidence of spatial perceptual variety amoung complex objects. The study of directional objects using the wavefield approach also supports the hypothesis. For both practical and creative applications it would be desirable to find a way to accurately represent a complex source and encode it into Ambisonic B-format. The conversion from source encoding to Ambisonic encoding depends on the location and orientation desired of the source. From a single source encoding, that source can be rendered anywhere and in any orientation around the listener. Figure 1 illustrates this scheme. The advantage of Ambisonic modularity is apparent here, in that we seek a process that encodes into a format that is independent of the rendering mechanism, whether it be a particular speaker array or headphones.[1] The wavefield approach lacks this intermediate stage.

The article is organized as follows. First the source representation is discussed, followed by the main part, the development of a method to transform a source encoding, with knowledge of its position and orientation, into

[1]See [10] for recent related work by the authors concerning the rendering of Ambisonic material onto headphones

an Ambisonic encoding. Some simulations are provided for verification and illustration. Finally we consider how the approach can be adapted for the Ambisonic encoding of reverberation depending on source and listener positions and orientations.

2 Source Representation

We wish to use a representation which can encode any source to any desired accuracy, relates well to direct observations of the field, and can be manipulated efficiently. The following possibilities suggest themselves. A source can be modelled with several monopoles. This would be appropriate if it actually has this structure, or because a rough and fast model is required. The source can be positioned and orientated using standard cartesian transformations. For more accuracy we can attempt to use many monopoles distributed over the source volume or surfaces. It is far from obvious how this would be done for a general source. Such a representation contains considerable redundancy since it describes the structure of the object as well as the sound produced.

2.1 The exterior harmonic expansion

Multipoles in their original form consist of infinitesimal arrangements of monopole sources. A multipole of sufficient order can represent a given field around an object arbitrarily well. Although they are operated on by simple cartesian operations, their infinitesimal nature does not lend itself to direct numerical manipulation. Also the relationship of multipole parameters to the directionality of the field rapidly increase in complexity with order. Closely related is the *exterior expansion* for the wave equation. This has basis functions in the frequency domain using spherical coordinates, $h_m(kr)Y_{mn}(\theta, \delta)$, where $h_m(kr)$ are the spherical hankel functions of the second kind, [11]. m is the multipole order of each function, and $k = 2\pi/\lambda$ is the wavenumber. The type of hankel function chosen gives an outward moving wave when associated with a positive frequency time piece $e^{i\omega t}$, the same convention used in [5].

An infinitesimally defined multipole of order m can always be expressed exactly using an exterior expansion with terms up to order m. For this reason an exterior expansion is alternatively called an *exterior multipole expansion* or just a *multipole*, [12]. Another term used is *singular expansion*, since the

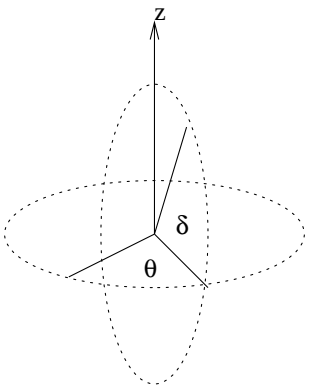

Figure 2: Spherical coordinates used.

center of the expansion has a singularity. The exterior expansion relates closely to the non-uniform directivity of a source, as discussed below, and our principal goal shall be to manipulate it to provide an Ambisonic source encoding. By multipole we shall mean an exterior expansion, unless otherwise stated.

The remainder of this section reviews the exterior expansion and introduces the conventions that will be used. In keeping with the high-order Ambisonic literature the real-valued N3D spherical harmonic set will be used throughout, [13, 5]. The components are defined for $m \geq 0$ and $m \geq n \geq 0$ by

$$Y_{mn}^{\sigma\ (N3D)}(\theta, \delta) = \sqrt{2m+1}\ \tilde{P}_{mn}(\sin\delta) \times \begin{cases} \cos n\theta & \text{if } \sigma = +1 \\ \sin n\theta & \text{if } \sigma = -1 \end{cases} \tag{1}$$

$$\tilde{P}_{mn}(\sin\delta) = \sqrt{(2-\delta_{0,n})\frac{(m-n)!}{(m+n)!}}\ P_{mn}(\sin\delta) \tag{2}$$

For $n = 0$, σ only takes the value $+1$. θ here measures the angle around the coordinate symmetry axis. $\pi/2 - \delta$ is the angle between the axis and the coordinate direction, so that δ would normally be called the elevation, as shown in Figure 2. The symmetry axis is normally called the z axis, which is not neccessary, but aids labeling in diagrams.

We shall use a slightly simplified notation that removes σ by extending n to negative values as used in more conventional harmonic sets,

$$Y_{mn} = \begin{cases} Y_{mn}^{+1} & \text{if } n \geq 0 \\ Y_{m|n|}^{-1} & \text{if } n < 0 \ . \end{cases} \tag{3}$$

For convenience we define coefficients, $O_{mn}(k)$, by a general exterior expansion,

$$p(\boldsymbol{r}, k) = k \sum_m i^{-m-1} h_m(kr) \sum_n Y_{mn}(\theta, \delta) O_{mn}(k) \ , \tag{4}$$

so that in the farfield where $h_m(kr)$ tends to $i^{m+1} e^{-ikr}/kr$, the field becomes

$$p_{far} = \frac{e^{-ikr}}{r} \sum_{m,n} Y_{mn}(\theta, \delta) O_{mn}(k) \ . \tag{5}$$

The $O_{mn}(k)$ coefficients then directly express the non-uniform directivity in this regime, where locally the field tends to an outward moving plane wave. In the the $O_{mn}(k)$ coincide with the *O-format* encoding used previously for Ambisonic synthesis, [3, 4]. The same name will be used here for the more general case described by (4). We emphasize that this is just a convention, for convenience and appropriate to its context, in the same sense as B-format is defined. Nothing essentially new is added.

$O_{mn}(k)$ can be readily calculated from measurements of the field on a sphere at any radius r outside the source region. Applying an integral over the sphere, $\int d\Omega \ Y_{mn}(\theta, \delta)$ to (4) gives

$$O_{mn}(k) = \frac{i^{m+1} \int d\Omega \ Y_{mn}(\theta, \delta) p(\boldsymbol{r}, k)}{4\pi k h_m(kr)} \ . \tag{6}$$

For a real object the field could be measured approximately with pressure microphones placed located on a sphere a fixed distance from the source. In the farfield where the field becomes planar, inwardly pointing directional mics are equally effective given the appropriate equalization including phase. For devices such as loudspeakers that convert electricity to sound linearly, the process can be simplified by repeated response measurements with a single mic that is moved. Speaker simulations might for instance be useful in high-end architectural simulations. When the $O_{mn}(k)$ responses are convolved with input signals for the speakers, the expansion signals are generated.

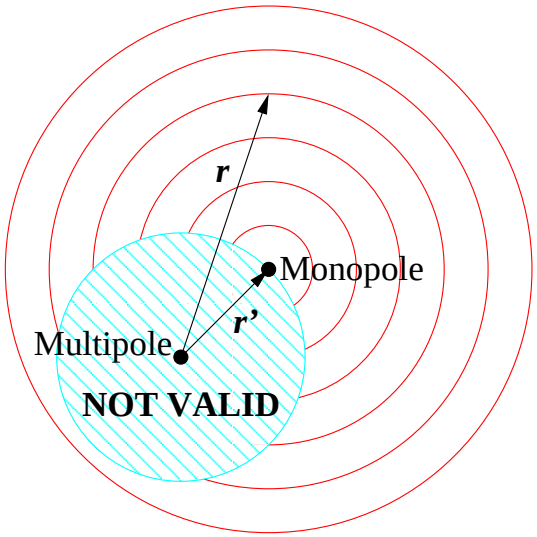

Figure 3: Multipole representation of a monopole.

2.2 Source approximation order and error

We consider now the order to which a source is approximated, m_{max}. We wish to minimize this subject to reconstruction error constraints. A source can be arbitrarily small and still have power up to any multipole order, for example using the explicit definition of infinitesimal multipoles. However this is unusual in a real acoustic source because opposed component sources are not usually found very close together. To gain insight into the more usual case, we examine multipole fields for a source consisting of a monopole offset from the expansion centre. A monopole source at position $\boldsymbol{r'}$ has the following multipole expansion in $\boldsymbol{r}$ about the origin, valid for $r > r'$, [11],

$$\frac{e^{-ik|r-r'|}}{|r-r'|} = ik \sum_{m=0}^{\infty} j_m(kr') h_m(kr) \sum_{n=-m}^{m} Y_{mn}(\theta', \delta') Y_{mn}(\theta, \delta) \qquad (7)$$

$j_m(kr')$ is the spherical Bessel function of the first kind. The arrangement is illustrated in Figure 3.

Figures 4 and 5 show some cross-sectional plots of $Re(p)/|p|$, for different orders and offset $r' = 2\lambda$, where $\lambda = 2\pi/k$ is the wavelength. Only one half the plane is shown because the field is symmetric about the line from multipole to monopole. The nearfield resolves sharply as the order is increased.

For order $m_{max} \approx 2\pi r'/\lambda = kr'$, the relative error compared with a real monopole is $< 1\%$ for $r > r' + \lambda$. Detailed error analysis of the multipole approximation, [12], agree with these observations, and fast convergence is cited as one of the key attributes of the spherical multipoles.

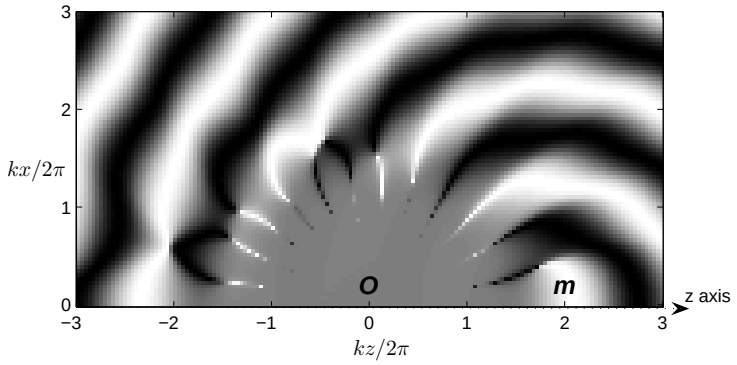

Figure 4: Multipole approximation, center **O**, of a displaced monopole, center **m**, $r' = 2\lambda$, $m_{max} = 12$. The cross-section is $\theta = 0$. x, z are cartesian coordinates in length units.

Rewriting for m_{max} that will ensure good reconstruction of a field from a region of diameter d, up to frequency, f_{max}, we find $m_{max} = \pi d f_{max}/c$. For example, frequencies up to 1500 Hz from an object 1 m width can be approximated well with $m_{max} = 14$. If we do not require good construction close to the limit $r = r'$, then the order can be reduced further. The farfield accuracy is not of so much interest, since at all orders the farfield tends locally to a plane wave. This can be conventionally encoded in Ambisonics using $B_{mn} = Y_{mn}(\theta_s, \delta_s)p(k)$, where the direction is to the source and $p(k)$ is the pressure from the source measured at the listener. Increasing the multipole order in this approximation can provide good reconstruction in the farfield, but not the nearfield.

For a general source with diameter d, we cannot expect to use a lower order than the displaced monopole example for similar accuracy, because

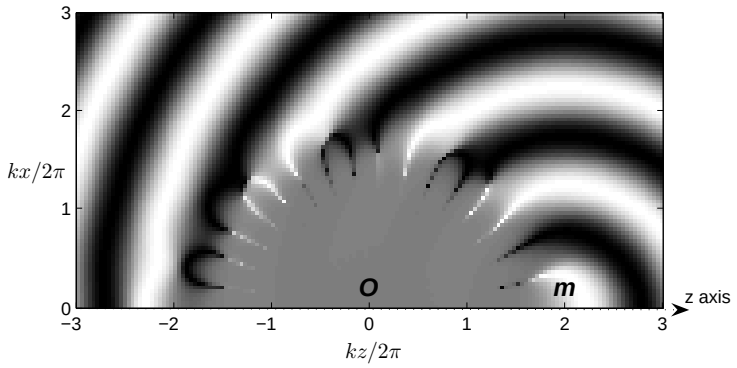

Figure 5: Multipole approximation, center **O**, of a displaced monopole, center **m**, $r' = 2\lambda$, $m_{max} = 16$. The cross-section is $\theta = 0$. x, z are cartesian coordinates in length units.

it would be unusual that different parts of the object would cancel out at higher orders. Conversely we wouldn't expect higher orders to be required, because that would require even more cancellation in order to make higher orders relatively significant. In summary, the formula for m_{max} provides a first estimate for the order required to represent the nearfield of a general object, although this is not true across all possible sources.

2.3 Multi-resolution sources

So far we have considered using single multipole expansions. In some cases a hybrid approach may be more appropriate, in which a source is represented using a several multipoles. This is neccessary whenever we wish to find the field at a free space inside the bounding sphere of an object, for example nearer to a table surface than its length. Outside the total bounding sphere a single multipole is sufficient. As we move closer to some part of the source more multipoles are neccessary. Far from the object compared to its size the field can be approximated as a plane wave, using the O-format coefficients to

determine the direction dependence. This scheme of successive simplification resembles the multi-resolution techniques common in computer graphics, [14].

3 Ambisonic encoding of multipoles

High-order Ambisonics is founded on the *interior expansion* that we shall also call the *freefield expansion* here, to emphasize that it is used to describe a sourceless region around the listener. Eq. (8) is the version of the expansion using N3D harmonics, $Y_{mn}(\theta, \delta)$, and defines the B-format coefficents, $B_{mn}(k)$, [5]. The expansion converges quickly on any source-free field, upto a given radius r. The typical order required to achieve 1% convergence is $m_{max} \approx kr$, [12].

$$p(\boldsymbol{r}, k) = \sum_m i^m j_m(kr) \sum_n Y_{mn}(\theta, \delta) B_{mn}(k) \tag{8}$$

3.1 Monopole encoding

For fields containing sources it is still possible to create a freefield expansion, however is only valid within a region that does not contain any source. Consider first a field containing a single monopole set away from the freefield expansion center. Eq. (7) can be recast as the freefield expansion for a monopole, by fixing $\boldsymbol{r}$ and instead varying $\boldsymbol{r}'$. The form of this expansion is then consistent with Eq. (8), from which the values of the $B_{mn}(k)$ can be read off, as shown in [5]. The condition of convergence $\boldsymbol{r}' < \boldsymbol{r}$ now implies that the expansion converges *within* a circle that just touches the monopole source. Figure 6 shows a field plot for such a monopole reconstructed to the 13th order, and set at a distance 2λ from the expansion center. Outside this area the expansion is a valid freefield, although no longer matches the source field. Overall convergence behaviour within the valid region is like any other freefield, although close to the monopole, $\delta < \lambda$, the order required to achieve a given error is increased compared to a smooth freefield, as we would expect, [12]. The limit set to the region of freefield convergence by the source can not be exceeded by increasing the freefield order.

Higher multipole sources have similar freefield expansions, since they can be generated as composites of infinitesimal monopoles. The convergence condition is then that the freefield expansion is valid within a radius that does not include any of the source.

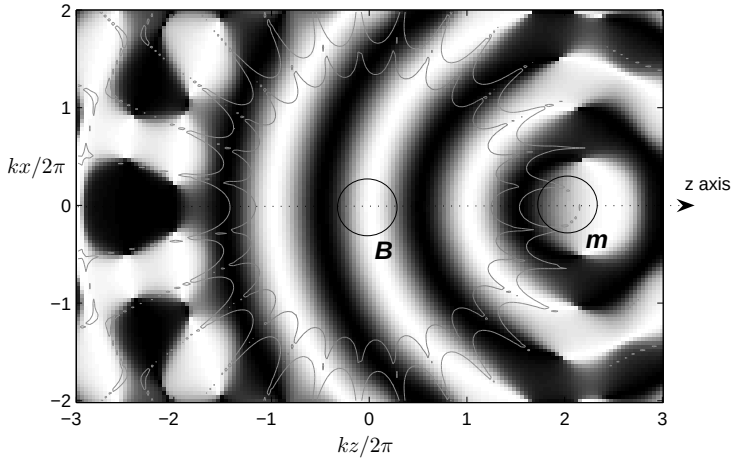

Figure 6: Cross-section of a field plot for a 13th order freefield expansion, center at **B**, of a monopole, center **O**. Error contours are shown at the 1% and 10% levels. The cross-section is $\theta = 0$. x, z are cartesian coordinates in length units.

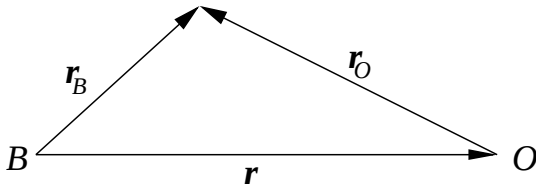

Figure 7: Vector notation

3.2 Multipole to freefield coefficient transformation

The main task in this section is to find $B_{mn}(k)$ in the presence of a multipole described by $O_{mn}(k)$ at a given position. It would be desirable to find a generalized closed form expression, as for the monopole case in [5]. However, it is not very apparent how this could be done or even if it would be the most practical method of calculation, so instead a more pragmatic approach is adopted yielding eventually a manageable integral expression. To begin (8) and (4) are equated. The notation is modified according to Figure 7,

$$\sum_m i^m j_m(kr_B) \sum_n Y_{mn}(\theta_B, \delta_B) B_{mn}(k) = k \sum_m i^{-m-1} h_m(kr_O) \sum_n Y_{mn}(\theta_O, \delta_O) O_{mn}(k) \tag{9}$$

To isolate $B_{mn}(k)$ the operator $\int d\Omega_B \; Y_{m'n'}(\theta_B, \delta_B)$ is applied, with r_B a freely chosen constant, and θ_O, δ_O and r_O are functions of the vector $\boldsymbol{r}_B$, yielding

$$4\pi i^{m'} j_{m'}(kr_B) B_{m'n'}(k) = k \sum_m i^{-m-1} \sum_n O_{mn}(k) \int d\Omega_B \; Y_{m'n'}(\theta_B, \delta_B) Y_{mn}(\theta_O, \delta_O) h_m(kr_O). \tag{10}$$

Relabeling indices, $B_{mn}(k)$ can be written as

$$B_{mn}(k) = \sum_{m',n'} M_{mnm'n'}(k, \boldsymbol{r}) O_{m'n'}(k), \tag{11}$$

where the filter matrix $M_{mnm'n'}(k, \boldsymbol{r})$ is

$$M_{mnm'n'}(k, \boldsymbol{r}) = \frac{k i^{-m-m'-1}}{4\pi j_m(kr_B)} \int d\Omega_B \; Y_{mn}(\theta_B, \delta_B) Y_{m'n'}(\theta_O, \delta_O) h_{m'}(kr_O). \tag{12}$$

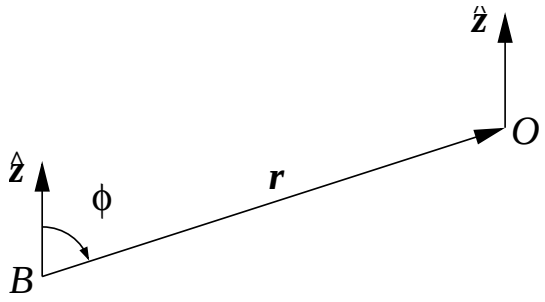

Figure 8: Finding components relative to $\boldsymbol{r}$

The $\boldsymbol{r}$ direction dependence in the matrix can be factored out by transforming the components $B_{mn}(k)$ and $O_{mn}(k)$ so they are relative to $\boldsymbol{r}$. Figure 8 shows the relationship between the initial coordinate axis, $\hat{\boldsymbol{z}}$, and the vector, $\boldsymbol{r}$, connecting the centres B and O. $\phi = \pi/2 - \delta$ together with θ specify a rotation mapping $\hat{\boldsymbol{z}}$ onto $\boldsymbol{r}$, written in components as $R_{m'n'n}(\theta, \phi)$. The third degree of freedom is unspecified, although it must be consistent. Therefore $R_{m'n'n}(\theta, -\phi)$ transforms $B_{mn}(k)$ and $O_{mn}(k)$ to find their coordinates relative to $\boldsymbol{r}$,

$$B'_{m'n'}(k) = \sum_n R_{m'n'n}(\theta, -\phi) B_{m'n}(k) \tag{13}$$

$$O'_{m'n'}(k) = \sum_n R_{m'n'n}(\theta, -\phi) O_{m'n}(k) \tag{14}$$

Now Eq. (11) can be written with an $\boldsymbol{r}$-direction-independent matrix, $M_{mnm'n'}(k, r)$,

$$B'_{mn}(k) = \sum_{m',n'} M_{mnm'n'}(k, r) O'_{m'n'}(k), \tag{15}$$

where

$$M_{mnm'n'}(k, r) = \frac{k i^{-m-m'-1}}{4\pi j_m(kr_B)} \int d\Omega_B \; Y_{mn}(\theta_B, \delta_B) Y_{m'n'}(\theta_O, \delta_O) h_{m'}(kr_O). \tag{16}$$

The coordinates in the integral are now relative to $\boldsymbol{r}$, although they haven't been relabeled. The symmetry this brings, with r_O independent

of $\theta_B = \theta_O$, can be used to factor the integral into a product of θ and δ integrals. To make this clear $Y_{mn}(\theta, \delta)$ is factored into

$$Y_{mn}(\theta, \delta) = \hat{P}_{mn}(\sin\delta) \times \begin{cases} \sqrt{2}\cos n\theta & \text{if } n > 0 \\ 1 & \text{if } n = 0 \\ \sqrt{2}\sin n\theta & \text{if } n < 0 \end{cases} \tag{17}$$

where for convenience later, $\hat{P}_{mn}$ is defined,

$$\hat{P}_{mn}(\sin\delta) = \sqrt{(2m+1)\frac{(m-|n|)!}{(m+|n|)!}}\, P_{m|n|}(\sin\delta) \tag{18}$$

and $P_{mn}(x)$ is the associated Legendre polynomial. (16) becomes

$$\begin{aligned} M_{mnm'n'}(k,r) &= \frac{ki^{-m-m'-1}}{4\pi j_m(kr_B)} \int d\delta_B \ \cos\delta_B \hat{P}_{mn}(\sin\delta_B)\hat{P}_{m'n'}(\sin\delta_O)h_{m'}(kr_O) \times 2\pi\delta_{nn'} \\ &= \frac{\delta_{nn'}ki^{-m-m'-1}}{2j_m(kr_B)} \int_{-1}^{+1} ds_B \hat{P}_{mn}(s_B)\hat{P}_{m'n'}(s_O)h_{m'}(kr_O), \end{aligned} \tag{19}$$

where $s_B = \sin\delta_B$ and $s_O = \sin\delta_O$. s_O and r_O can be found from r, r_B and s_B using $r_B s_B - r_O s_O = r$. $r_O = r\sqrt{1+\alpha^2 - 2\alpha s_B}$ and $s_O = r(\alpha s_B - 1)/r_O$, where $\alpha = r_B/r$. Setting $\alpha = .51111$ ensures good numerical behaviour.

Eq. (15) can now be simplified using,

$$B'_{mn}(k) = \sum_{m,n} \frac{1}{r} M_{mnm'}(kr) O'_{m'n}(k), \tag{20}$$

where we define a simplified matrix coefficient with 3 indices rather than 4.

$$M_{mnm'}(k) = \frac{ki^{-m-m'-1}}{2j_m(r_B)} \int_{-1}^{+1} ds_B \hat{P}_{mn}(s_B)\hat{P}_{m'n}(s_O)h_{m'}(r_O), \tag{21}$$

with $r = k$ implicit. Clearly this is defined only for $n < m$ and $n < m'$. This means for a given source the number of filters increases only linearly with B-format order required. The new filter coefficients are given in terms of one parameter, k. The actual filter acting in (20) is scaled in frequency by the radius r and there is a distance factor $1/r$. Putting this together with (13) gives $B_{mn}(k)$ in terms of $O_{mn}(k)$,

$$B_{mn}(k) = \sum_{n'} R_{mnn'}(\theta, \phi) \sum_{m'} \frac{1}{r} M_{mn'm'}(kr) \sum_{n''} R_{m'n'n''}(\theta, -\phi)\ O_{m'n''}(k) \tag{22}$$

Note that an orientation rotation could be incorporated into the first rotation acting on O_{mn}.

3.3 Validation and properties

To provide an immediate confidence test that the derived formulas are correct, a random test 5th order multipole was constructed, shown in Figure 9, and compared with the 13th order freefield expansion calculated using the matrix (22), shown in Figure 10. The error contours in Figure 10 at 10% and 1% levels are for deviations from the original multipole shown in Figure 9. The region of agreement extends as far as the center of the original multipole, as expected, and indicates that the calculations described in this section are correct.

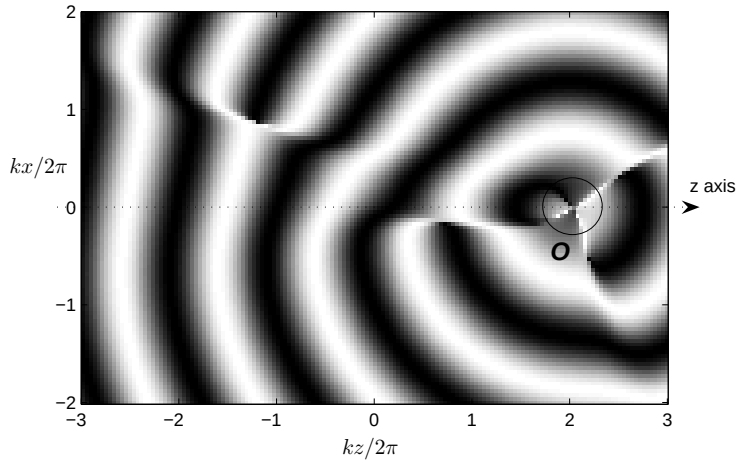

Figure 9: Cross-section of a field plot for a 5th order multipole, center at **O**. The cross-section is $\theta = 0$. x, z are cartesian coordinates in length units.

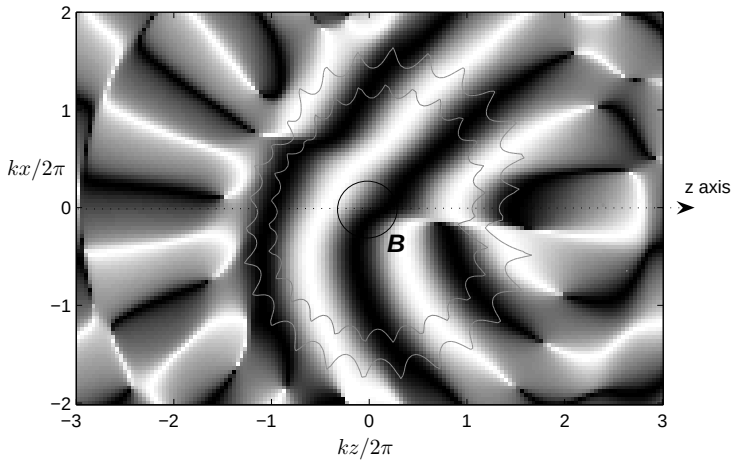

Figure 10: Cross-section of a field plot for a 13th order freefield expansion, center at **B**, of a multipole, center **O**. Error contours are shown at the 1% and 10% levels. The cross-section is $\theta = 0$. x, z are cartesian coordinates in length units.

Next we examine $M_{mnm'}(kr)$ by checking that it is consistent with previous results for the monopole case,[5], in which the encoded signal is given by $B_{mn} = S(k)F_m(kr)Y_{mn}(\theta, \delta)$, where $F_m(kr) = i^{-m}h_m(kr)/h_0(kr)$. To match the alignment used to define $M_{mnm'}(kr)$, $\theta = \delta = \pi/2$. We first note that the source term $S(k)$ includes the delay and distance attenuation so that $S(k) = \frac{e^{ikr}}{r}O_{00}(k)$. In order to isolate the part matching $F_m(kr)$, we look at the adjusted value, $M_{m00}(kr)/(e^{-ikr}/r)/Y_{m0}(0, \pi/2)$. With $r = 1$, this produces the plots shown in Figure 11, matching previous results, [5]. Further plots reveal how M extends to encode higher multipoles. The general picture is that with the e^{-ikr}/r piece factored out, the response is always minimum phase. For small k the order of the filter becomes $m + m'$, while for large k it is n. The transition occurs around $k = 2$ corresponding to ≈ 0.3 wavelength separation from the source. $M_{mnm'}(kr)$ has symmetries which reduce the computational cost of using it; $M_{mnm'}(kr) = M_{m'nm}(kr)(-1)^{m+m'} = M_{m-nm'}(kr)$. The first of these is useful for cross checking the accuracy of value, since the integrals are quite different. Figure 12 is an example showing the am-

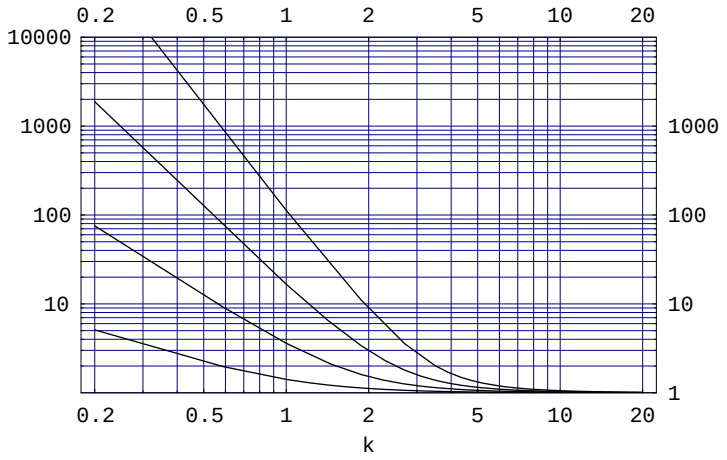

Figure 11: Amplitude response for $M_{m00}(kr)/(e^{-ikr}/r)/Y_{m0}(0,\pi/2)$, $m = 1,2,3,4$

plitude response for $M_{211}(kr)/(e^{-ikr}/r)$ along with $kM_{211}(kr)/(e^{-ikr}/r)$ to make clear the large k behaviour clear. Figure 13 shows the corresponding phase response. Another example, with $n = 2$, is shown in Figures 14 and 15.

In [5] filters were commuted from the decoding stage to control the large amplitudes at low values of k. The situation at first appears worse here because filters encoding high multipoles can have much higher order for the same order m of the B-format encoding. However, at the values of k where the filters grow large, the size of the source object in wavelengths becomes small, and a lower source order suffices to approximate it well, according to the discussion in Section 2 where a regular source is considered. This means that low frequencies can be filtered out progressively from the higher orders of object encoding, so avoiding excessive gains. The filtering should be performed dynamically according to distance. The highest order retained, m_{max} is determined by the highest frequency, f_{max}, that is required to be accurately reconstructed, as described in Section 2. For an accurately constructed field of sufficiently low frequency, a monopole suffices.

We do not investigate the implementation of the filter matrix in detail here, but note that in general it will take a similar form to that described for the monopole case, [5]. Because the filters are evaluated numerically,

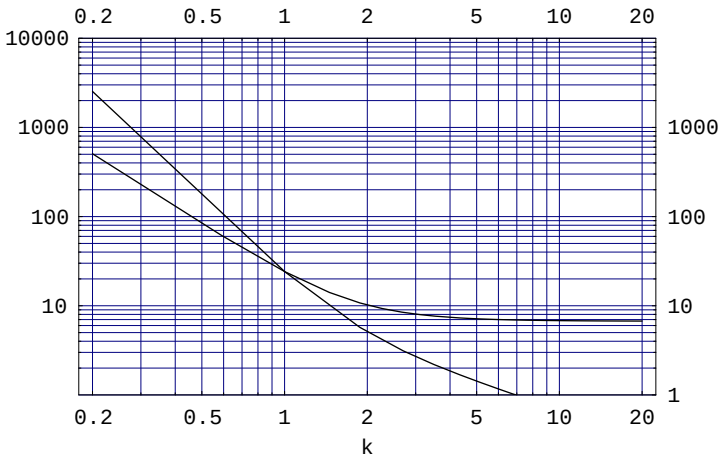

Figure 12: Amplitude response for $M_{211}(kr)/(e^{-ikr}/r)$ and $kM_{211}(kr)/(e^{-ikr}/r)$

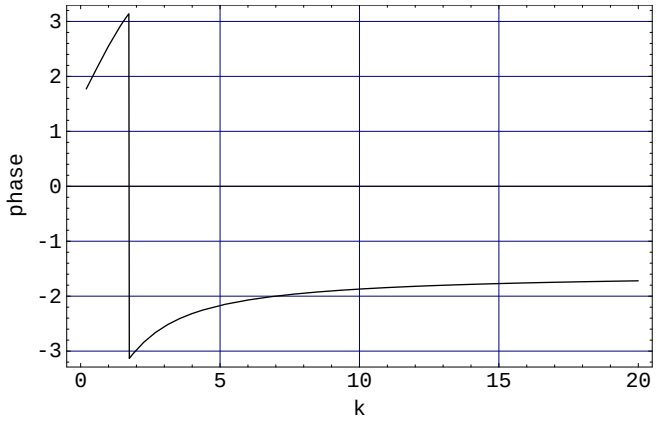

Figure 13: Phase response for $M_{211}(kr)/(e^{-ikr}/r)$

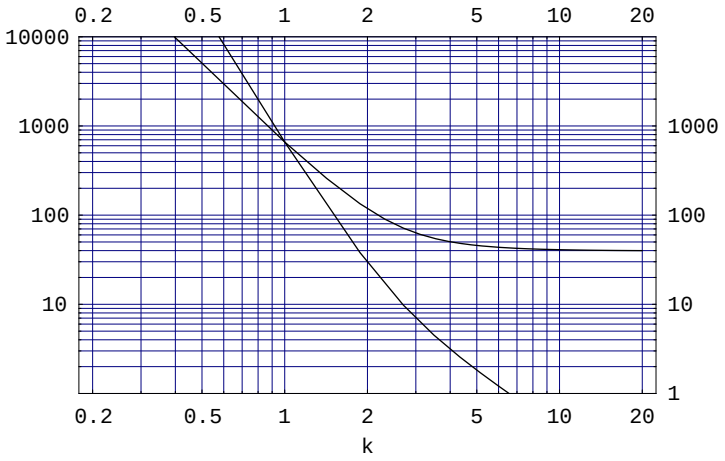

Figure 14: Amplitude response for $M_{223}(kr)/(e^{-ikr}/r)$ and $k^2 M_{223}(kr)/(e^{-ikr}/r)$

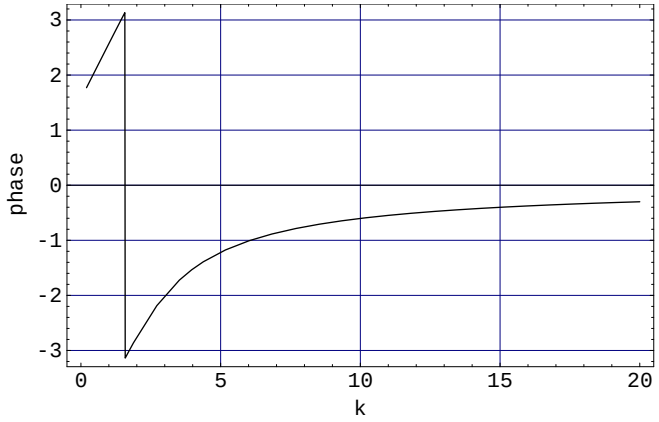

Figure 15: Phase response for $M_{223}(kr)/(e^{-ikr}/r)$

they must be converted to IIR form by pole/zero fitting. Filter modification according to radius can then achieved by scaling the poles and zeros in frequency.

4 Reverberation encoding and transformation

This article has focused on the synthesis of the direct signal from complex objects in the nearfield. Related techniques can be applied to the synthesis of a reverberant signal originating from a complex source.

4.1 Encoding source directivity in reverberation

Conventional room responses are mono to mono, or mono to multichannel, where multichannel could include B-format. This means that the reverberant sound from a source is the same no matter how it is oriented, where as real reverberation can vary considerably. Using a harmonic matrix of the form Eq. (12) it is possible, because of linear supposition, to fully encode the reverberant response to source directivity, for a given pair of source and listener positions. For a source described by $O_{m'n'}(k)$ and a listening field by $B_{mn}(k)$,

$$B_{mn}(k) = \sum_{m',n'} M^{rev}_{mnm'n'}(k, \boldsymbol{x}_B, \boldsymbol{x}_O) O_{m'n'}(k) \quad , \tag{23}$$

where $\boldsymbol{x}_B$ and $\boldsymbol{x}_O$ are the position vectors of the listener and source. The $M^{rev}_{mnm'n'}$ could be measured in a real space using directional sources and directional microphones, measuring the response on each microphone component for each source component. There are many ways this could be achieved, but in any case the directional components must be able to cover the desired order of spherical harmonic resolution. The order of the source components is not so important compared to the order of the microphones, since the latter must support the spatial resolution in the listener's hearing. A small source order increase is expected to deliver a considerable advantage over the conventional zero order source. The encoding of source directivity could be particularly valuable in an interactive application where the listener controls the orientation of a sound source, and so can probe the surrounding acoustic. $M^{rev}_{mnm'n'}$ could also be calculated offline by applying the source-microphone technique to simulations using ray-tracing or other models.

4.2 Transforming reverberation with listening position

A modified matrix technique can be used to transform reverberation according to a change of listening position. This allows a single $M^{rev}_{mnm'n'}$ to be used for a range of listener positions, by transforming B_{mn} from Eq. (23) to the reverberant signal at the new position, $B'_{mn}(k)$. In [15] there is a partial description of this method. The first pressure or zero-order component of the reverberant signal is found everywhere in a room using a single expansion. Here we reproduce the full high-order directional qualities of reverberation about any point. Reworking the previous calculations leading to Eq. (21) produces the following result in terms of a new matrix $M^{BB}_{mnm'}$,

$$B'_{mn}(k) = \sum_{n'} R_{mnn'}(\theta, \phi) \sum_{m'} \frac{1}{r} M^{BB}_{mn'm'}(kr) \sum_{n''} R_{m'n'n''}(\theta, -\phi)\ B_{m'n''}(k) \quad , \tag{24}$$

where

$$M^{BB}_{mnm'}(k) = \frac{k i^{m'-m}}{2 j_m(r'_B)} \int_{-1}^{+1} ds_B \hat{P}_{mn}(s'_B) \hat{P}_{m'n}(s_B) j_{m'}(r_B) \quad , \tag{25}$$

with r'_B, s'_B, r_B and s_B replacing r_B, s_B, r_O and s_O respectively. To verify this, a random 12th order field B_{mn} has been synthesized, shown in Figure 16, and transformed using Eq. (24) to an 18th order field B'_{mn} centered at a distance 2λ from B_{mn}, shown in Figure 17. The error contours show clear agreement which extends beyond the center of B_{mn} to a radius r where $kr \approx m_{max} = 18$, as expected. As noted previously, when transforming a multipole source it is not possible to extend beyond the original center in this way.

This technique can reproduce high definition spatialized reverberation more efficiently than by direct simulation with ray tracing and similar methods, since the computational complexity is limited by the reconstruction order and not the complexity of the simulation.

5 Conclusion

A method has been presented for encoding a general acoustic source, and transcoding it to a high-order Ambisonic signal, dependent on source orientation, and position relative to the listener. The method also lends itself to

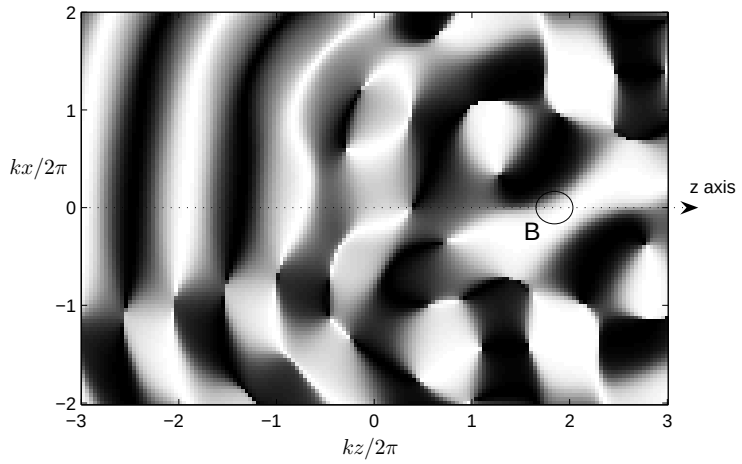

Figure 16: Cross-section of a field plot for a 12th order freefield harmonic expansion, center at **B**. The cross-section is $\theta = 0$. x, z are cartesian coordinates in length units.

the direct measurement of real sources using an array of surrounding microphones. The approach is considerably more elaborate and costly than plane wave or monopole synthesis, however it is expected that in the context of complex sources displayed with a high-quality rendering system, the efforts are worthwhile. Related results have been presented for the generation and transformation of reverberation. Future realizations will investigate further.

References

[1] M.A. Gerzon. Ambisonics in multichannel broadcasting and video. *Journal of the Audio Engineering Society*, 33:859–871, 1985.

[2] M.A. Gerzon. General metatheory of auditory localisation. In *92nd AES Convention Preprints*, 1992.

[3] D. Menzies. *New Performance Instruments for Electroacoustic Music*. PhD thesis, University of York, UK, 1999.

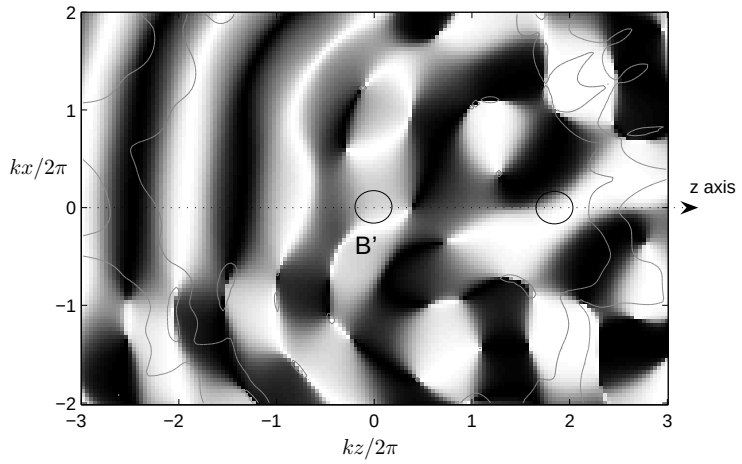

Figure 17: Cross-section of a field plot for a 18th order freefield expansion, center at **B'**, of a freefield, center **B** shown in Figure 16. Error contours are shown at the 1% and 10% levels. The cross-section is $\theta = 0$. x, z are cartesian coordinates in length units.

[4] D. Menzies. W-panning and o-format, tools for object spatialisation. In *Proc. AES 22nd International Conference*, 2002.

[5] J. Daniel. Spatial sound encoding including near field effect. In *Proc. AES 23nd International Conference*, 2003.

[6] A.J. Berkhout, D.d. Vries, and P. Vogel. Acoustic control by wave field synthesis. *J. Acoust. Soc. Am.*, 93:2764–2778, 1993.

[7] J. Daniel, R. Nicol, and S. Moreau. Investigations of high order ambisonics and wavefield synthesis for holophonic sound imaging. In *AES 114th Convention Preprints*, 2003.

[8] T. Caulkins, E. Corteel, and O. Warusfel. Synthesizing realistic sound sources in wfs installations. In *Proc. DAFX04*, 2004.

[9] O. et al. Warusfel. Reproduction of sound source directivity for future audio applications. In *Proc. International Congress on Acoustics*, 2004.

[10] D. Menzies and M. Al-Akaidi. Nearfield binaural synthesis. *J. Acoust. Soc. Am.*, In press.

[11] P.M. Morse and K.U. Ingard. *Theoretical Acoustics*. McGraw-Hill, 1968.

[12] N. A. Gumerov and R. Duraiswami. *Fast multipole methods for the Helmholtz equation in three dimensions*. Elsevier Science, 2005.

[13] J. Daniel. *Représentation de Champs Acoustiques, Application la Transmission et à la Reproduction de Scnes Sonores Complexes dans un Contexte Multimdia*. PhD thesis, University of Paris 6, Paris, France, 2000.

[14] M. S. Dodgson, N. A.and Floater and M. A. (Eds.) Sabin. *Advances in Multiresolution for Geometric Modelling*. Springer, 2005.

[15] R. Duraiswami, N. A. Gumerov, D. N. Zotkin, and L. S. Davis. Efficient evaluation of reverberant sound fields. 2001.